

# INTERMOLECULAR VIBRATIONS OF THE COMPLEX OF NO IN THE $ns\sigma$ RYDBERG STATES AND Ar

KAZUHIDE TSUJI, KAZUHIKO SHIBUYA and KINICHI OBI

*Department of Chemistry, Tokyo Institute of Technology, Ohokayama, Meguro,  
Tokyo 152, Japan*

*(Received 2 May, 1994)*

The resonance enhanced multiphoton ionization method has been applied to the study of NO-Ar van der Waals complex in the  $ns\sigma$  ( $n = 3,4$ ) Rydberg states. We have assigned the intermolecular vibrations appearing in the  $\tilde{A}-\tilde{X}$  excitation spectrum of the complex. The bending structure appeared only with the excitation of the stretching mode in the  $\tilde{A}$  state, which was interpreted by intermolecular forces. The  $\tilde{E}-\tilde{A}$  excitation spectra were independent of the initial intermolecular level in the  $\tilde{A}$  state and the dissociation threshold to  $\text{NO}(E^2\Sigma^+) + \text{Ar}$  was determined to be  $60950 \text{ cm}^{-1}$ . The  $s$ - $d$  mixing in the  $4s\sigma$  orbital would make the intermolecular vibrational structure in the  $\tilde{E}-\tilde{A}$  spectra complex.

KEY WORDS: NO, van der Waals Complex, Intermolecular potential, Rydberg state

## INTRODUCTION

Spectroscopy of the van der Waals (vdW) complexes is a powerful tool to study intermolecular and internuclear potential surfaces (IPS). It provides the precise information on not only the internuclear potentials but also angle dependent IPS in atom-diatomic molecule systems. The metal-rare gas (Rg) complexes in the Rydberg states have been well studied, and their IPS are strongly depend on both radial distribution of the Rydberg electron and internuclear distance, and successfully interpreted by charge-charge induced dipole interaction and exchange repulsion [1,2]. The IPS of HCl-Rg complexes, especially HCl-Ar, have recently been determined to be anisotropic in the ground state [3]. The experimental and theoretical studies [4] have extensively been carried out on the OH-Rg complex as an example of vdW complexes between open-shell molecule and closed-shell atom. It is found that the nature of the bond between OH and Ar is physical (dispersion and induction force) in the ground state and chemical (covalent in Ar-H-O geometry and charge-transfer in Ar-O-H geometry) in the  $\tilde{A}$  state.

The NO molecule is a typical open-shell species, and a series of the Rydberg states are well characterized spectroscopically. Especially, the lowest Rydberg state of NO,  $A^2\Sigma^+(3s\sigma)$ , is a pure Rydberg state free from perturbation by the valence

states [5,6]. The  $E^2\Sigma^+(4s\sigma)$  state belongs to the same Rydberg series ( $ns\sigma$ ) as the  $A^2\Sigma^+$  state. Concerning to molecular parameters, they have essentially the same rotational and centrifugal distortion constants, but only spin-rotation parameter is different [7]. Then, we can assume that they have the same spectroscopic character and only differ in the radial distribution of the Rydberg electron. Therefore, comparison of vibrational structures of NO-Ar in the  $\tilde{E}$  and  $\tilde{A}$  states gives information to investigate how IPS depends on the radial distribution of Rydberg electron.

The bound-free electronic spectrum of the NO-Ar vdW complex for the  $\tilde{A}-\tilde{X}$  transition was first measured by Langridge-Smith *et al.* [8]. Mills *et al.* [9] determined the T-shaped structure of the NO-Ar vdW complex in the ground state. In a recent paper, we have reported on the bound-bound MPI and photodissociation action spectra of the  $\tilde{A}-\tilde{X}$  transition [10]. We have determined the intermolecular distances and binding energies of the complex in both  $\tilde{A}$  and  $\tilde{X}$  states. The shape resonance peaks in the photodissociation action spectra have indicated the existence of the barrier in IPS. We can interpret that IPS between NO( $A^2\Sigma^+$ ) and Ar is mainly built up of the charge-charge induced dipole and electron exchange interactions.

In this paper, we measured the  $\tilde{A}-\tilde{X}$ ,  $\tilde{E}-\tilde{X}$ , and  $\tilde{E}-\tilde{A}$  excitation spectra using a resonance enhanced multiphoton ionization (REMPI) method. We assigned the bending structure of the  $\tilde{A}$  state. The dissociation threshold of the  $\tilde{E}$  state was determined.

## EXPERIMENT

The NO-Ar vdW complexes are generated in the molecular beam. The REMPI experiments were performed using a time-of-flight (TOF) mass spectrometer and a laser. The experimental setup used was described previously [10]. A pulsed supersonic valve (Jordan, PSV) was employed as a beam source. The sample gas of NO / Ar was premixed in a 10 l aluminum bottle. The total pressure was 1 to 7 atm and the fraction of NO was less than 1%. The molecular beam was introduced into an ionization room of the TOF tube and ionized by laser light crossed perpendicularly. The REMPI experiments were performed with dye lasers (Lumonics, HyperDYE-300, 0.1  $\text{cm}^{-1}$  resolution) pumped by the third or second harmonics of a Nd<sup>3+</sup>:YAG laser (Lumonics, HY750). The dye laser output was doubled with a crystal (Inrad, AUTO Tracker II). The ion signals measured by a microchannel plate were averaged by a gated integrator (Stanford Research, SR-250) and recorded on a strip chart recorder (Rikadenki, R-60). The signals were further digitized by an A/D converter installed in the strip chart recorder, and sent to a personal computer through GPIB.

## RESULTS AND DISCUSSION

Figure 1 shows the excitation schemes employed in this study. Figure 2(a) shows a two-color (1 + 1') REMPI excitation spectrum of the  $\tilde{A}-\tilde{X}$  transition of the NO-Ar vdW complexes. This spectrum is associated with the NO  $A^2\Sigma^+-X^2\Pi(O-O)$  transition. The strongest band A observed at 44242.4  $\text{cm}^{-1}$  is supposed to be the band origin,  $T_0(\text{NO-Ar})$ , which is blue shifted by 43.5  $\text{cm}^{-1}$  from the band origin of uncomplexed

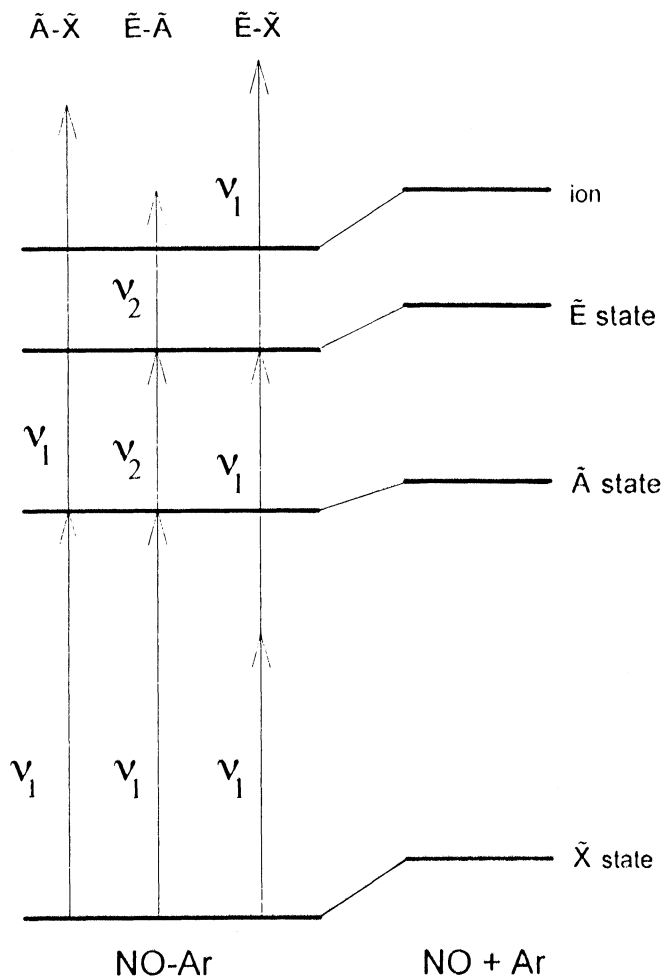
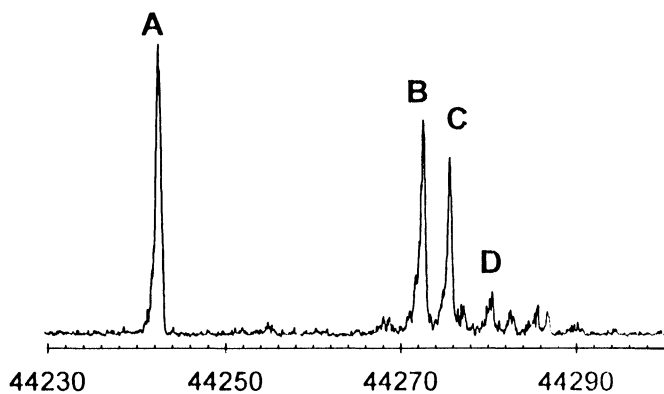


Figure 1. Excitation scheme.

NO. The high-resolution spectra of four bands labeled **A**, **B**, **C**, **D** are apparently red-shaded. The effective rotational constants were determined from rotational analysis of Bands **A**, **B**, and **C** using an empirical model based on the  ${}^2\Sigma-{}^2\Pi$  type transition, as listed in Table 1. In the case of NO-Ar, the effective rotational constant  $B_{\text{eff}}$  depends primarily on the intermolecular distance  $R_{\text{vdW}}$ . The  $R_{\text{vdW}}$  values estimated are also listed in Table 1.

There are two intermolecular vibrations in the atom-diatomic vdW complex; intermolecular stretch and bend. The intermolecular bending mode can be treated as near-free rotation of the diatomic molecule when the complex is weakly anisotropic [11], and the vibrational state is denoted as  $(\nu_{\text{NO}}, n^{|K|}, \nu_s)$ , where  $\nu_{\text{NO}}$  is the stretching vibrational quantum number of NO,  $n$  is the rotational quantum number of diatomic molecule which is quantized along the intermolecular axis with projection  $K$ , and  $\nu_s$

(a)  $\tilde{A}(0, n^k, v_s) - \tilde{X}(0, 0^0, 0)$ 

(b) Bending Structure

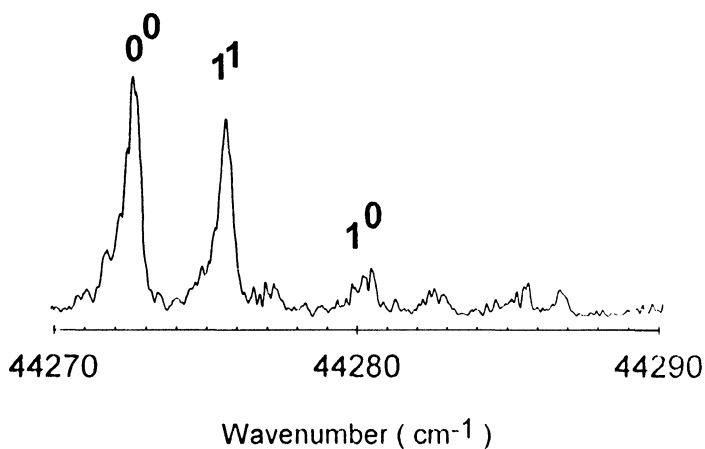


**Figure 2.** Two-color ( $1 + 1'$ ) REMPI excitation spectrum for the  $\tilde{A}(0, n^k, v_s) - \tilde{X}(0, 0^0, 0)$  transition of NO-Ar vdW complex. The  $\nu_2$  laser was fixed at  $32300 \text{ cm}^{-1}$ . The wavenumber indicates the transition energy of the  $\nu_1$  laser. (a) The overview spectrum. (b) The expanded spectrum of the bend-stretch combination bands. The bending quantum numbers are also indicated.

**Table 1** Rotational constants, intermolecular distances, and vibrational assignments in the  $\tilde{A}$  state of NO-Ar vdW complex.

<i>band</i>	<i>transition energy</i> ( $\text{cm}^{-1}$ )	<i>rotational constant</i> ( $\text{cm}^{-1}$ )	<i>intermolecular distance</i> ( $\text{\AA}$ )	<i>assignment</i>
<b>A</b>	44242.4	0.046	4.6	(0, 0 <sup>0</sup> , 0)
<b>B</b>	44272.6	0.035	5.3	(0, 0 <sup>0</sup> , 1)
<b>C</b>	44275.6	0.034	5.3	(0, 1 <sup>1</sup> , 1)
<b>D</b>	44280.3	–	–	(0, 1 <sup>0</sup> , 1)

is the intermolecular stretching vibrational quantum number of the complex. In the case of the NO ( $A^2\Sigma^+$ )–Ar complexes, the spin angular momentum may be negligible because NO in the  $A^2\Sigma^+$  state belongs to Hund's case (b).

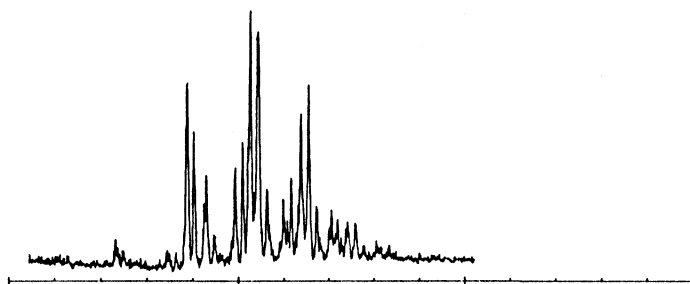
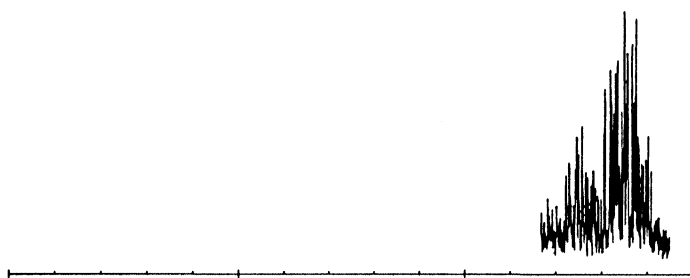
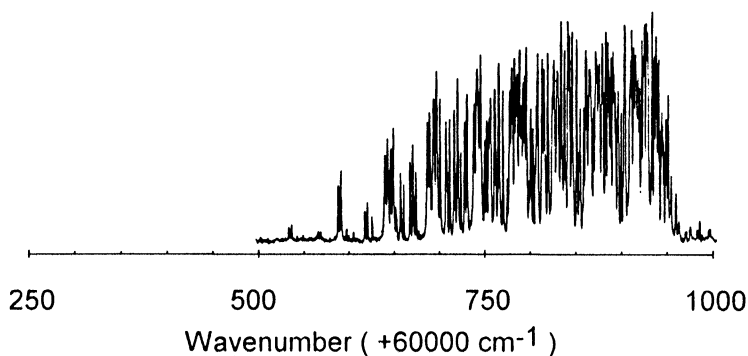
Bands **B**, **C**, and **D** in Fig. 2 show almost the same rotational contour and the intermolecular distances of the complex excited by Bands **B** and **C** are longer than that by Band **A** as listed in Table 1. These facts indicate that the intermolecular stretching mode contributes to three levels prepared by Bands **B**, **C**, and **D**. Therefore, Band **B** is thought to correspond to the transition to the intermolecular stretching fundamental level  $(0, 0^0, 1)$  in the  $\tilde{A}$  state, and the final states of Bands **C** and **D** seem to be the bend-stretch combination levels,  $\tilde{A}(0, 1^0, 1)$  or  $\tilde{A}(0, 1^1, 1)$ . Due to the T-shape geometry of NO-Ar [9], the  $1^1$  level lies lower than the  $1^0$  level [11]. Therefore, we assign Band **C** to the  $\tilde{A}(0, 1^1, 1) - \tilde{X}(0, 0^0, 0)$  transition and Band **D** to the  $\tilde{A}(0, 1^0, 1) - \tilde{X}(0, 0^0, 0)$  transition. The assignments are indicated in the last column in Table 1. The bending structure is also shown in Fig. 2(b).

In our previous paper [10], the molecular characteristics, such as smaller binding energy in the  $\tilde{A}$  state than that in the  $\tilde{X}$  state, are successfully interpreted using the two kinds of intermolecular forces, that is, the repulsive exchange interaction between the  $3s\sigma$  Rydberg electron of NO and the electrons of Ar, and attractive charge-charge induced dipole interaction between ion core of NO and Ar.

It seems strange that the pure bending band was not observed, although the stretch-bend combination bands (Bands **C** and **D**) were observed. The interpretation presented in the previous paper gives an answer to reply why the pure bending band was not observed. At short intermolecular distance which corresponds to no vibrational excitation of the intermolecular stretch, the charge-charge induced dipole interaction may be stronger and IPS is more anisotropic. Then, the intermolecular bending mode behaves like a normal bending vibration rather than a near-free rotation, and the progression would be very short.

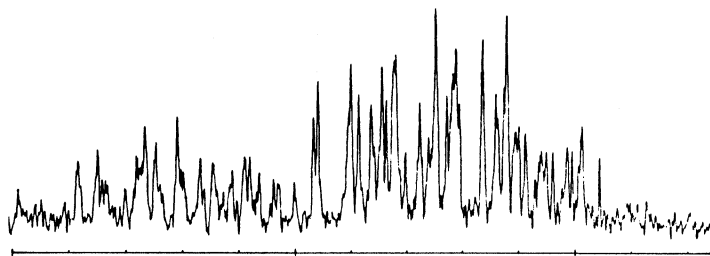
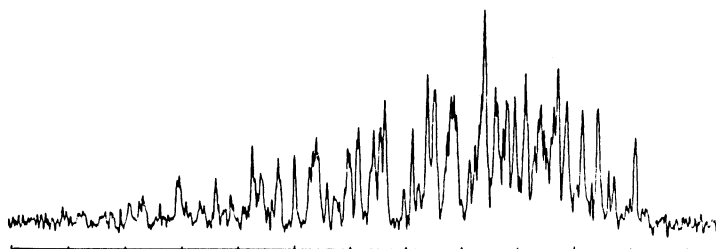
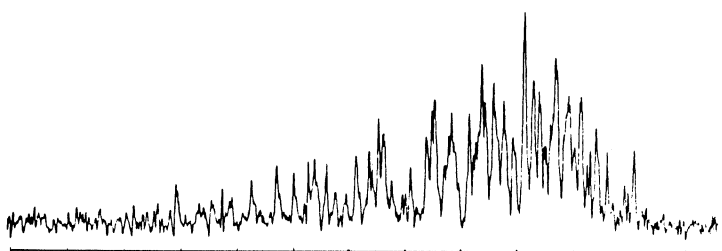
To confirm the interpretation described above, we investigated the  $\tilde{E}-\tilde{A}$  transition, where the  $\tilde{E}$  state corresponds to the  $4s\sigma$  Rydberg state of NO. The difference between the  $E^2\Sigma^+$  and  $A^2\Sigma^+$  states are only in the principal quantum number of the Rydberg electron, which reflects the change in the radial distribution of the Rydberg orbital. The intermolecular distance in the  $\tilde{A}$  state is comparable with the average radius of the  $3s\sigma$  Rydberg electron. In the case of NO( $E^2\Sigma^+$ )–Ar, the average radius of  $4s\sigma$  Rydberg electron is expected to be much larger than that of  $3s\sigma$ . Therefore, the Ar atom is situated inside the  $4s\sigma$  orbital, and the binding energy of the  $\tilde{E}$  state will be much larger than that of the  $\tilde{A}$  state.

Figure 3 (a) shows the  $(2 + 1)$  REMPI excitation spectrum for the  $\tilde{E}(0, n^k, v_s) - \tilde{X}(0, 0^0, 0)$  transition of NO-Ar vdW complexes, which has a complicated band structure due to intermolecular vibrations on the NO( $E^2\Sigma^+$ )–Ar IPS. The peak observed at the lowest wavenumber may be the 0–0 band (the upper limit), and is red-shifted by  $496.8\text{ cm}^{-1}$  from the origin of uncomplexed NO. Therefore, the binding energy for the  $\tilde{E}$  state is  $585\text{ cm}^{-1}$  (the lower limit) because the binding energy for the  $\tilde{X}$  state is  $88\text{ cm}^{-1}$  [10]. The binding energy for the  $\tilde{E}$  state is more than ten times as large as that for the  $\tilde{A}$  state. This fact is an experimental evidence to justify our interpretation on the intermolecular forces.

(a)  $\tilde{E}(0, n^k, v_s) - \tilde{X}(0, 0^0, 0)$ (b) Unsaturated  $\tilde{E}(0, n^k, v_s) - \tilde{A}(0, 0^0, 0)$ (c) Saturated  $\tilde{E}(0, n^k, v_s) - \tilde{A}(0, 0^0, 0)$ 

**Figure 3.** (2 + 1) REMPI excitation spectrum for the  $\tilde{E}(0, n^k, v_s) - \tilde{X}(0, 0^0, 0)$  transition and (1 + 1' + 1') REMPI excitation spectra for the  $\tilde{E}(0, n^k, v_s) - \tilde{A}(0, 0^0, 0)$  transition of NO-Ar vdW complex. The wavenumber indicates the transition energy of  $2\nu_1$  for (a), and  $\nu_1 (44242.4 \text{ cm}^{-1}) + \nu_2$  for (b) and (c).

The  $\tilde{E}-\tilde{A}$  excitation spectra were measured to probe a wide range of IPS. The  $\tilde{E}-\tilde{A}$  excitation spectrum provides the information on IPS around the intermolecular distance of 4.6 or 5.3 Å which is the intermolecular distance for the (0, 0<sup>0</sup>, 0) and (0, n<sup>k</sup>, 1) levels in the  $\tilde{A}$  state (see Table 1), while the  $\tilde{E}-\tilde{X}$  excitation spectrum provides that around  $R_{\text{vdW}} = 3.7$  Å. Figure 4 shows the  $\tilde{E}-\tilde{A}$  excitation spectra of the

(a)  $\tilde{E}(0, n^k, v_s) - \tilde{A}(0, 0^0, 0)$ (b)  $\tilde{E}(0, n^k, v_s) - \tilde{A}(0, 0^0, 1)$ (c)  $\tilde{E}(0, n^k, v_s) - \tilde{A}(0, 1^1, 1)$ 

850

900

950

Wavenumber ( +60000 cm<sup>-1</sup> )

**Figure 4.**  $(1 + 1' + 1')$  REMPI excitation spectra for the  $\tilde{E}(0, n^k, v_s) - \tilde{A}(0, n^k, v_s)$  transition of NO-Ar vdW complex. The initial states are (a)  $\tilde{A}(0, 0^0, 0)$ , (b)  $\tilde{A}(0, 0^0, 1)$ , and (c)  $\tilde{A}(0, 1^1, 1)$  levels.

NO-Ar complex where the initial intermolecular vibrational levels of the A state are the  $(0, 0^0, 0)$ ,  $(0, 0^0, 1)$  and  $(0, 1^1, 1)$  levels. In all the spectra, the probe laser power was as low as possible to avoid the saturation broadening, and the S/N ratio was rather low as the result.

All the  $\tilde{E}-\tilde{A}$  spectra shown in Figure 4 have the following characteristic features independent of the initial intermolecular vibrational levels. (1) The  $\nu_2$  wavenumbers measured consist in almost the same region as the  $E^2\Sigma^+ - A^2\Sigma^+$  (0—0) band of

uncomplexed NO (the band origin = 60863 cm<sup>-1</sup>). (2) The transition energy in the excitation via sequential  $\tilde{E}-\tilde{A}-\tilde{X}$  covers over only 50–100 cm<sup>-1</sup> (Fig. 4), which is much smaller than 300 cm<sup>-1</sup> in the excitation via direct  $\tilde{E}-\tilde{X}$  (Fig. 3 (a)). (3) The level density probed by the  $\tilde{E}-\tilde{A}$  transition is much higher than that probed by the  $\tilde{E}-\tilde{X}$  transition. Based on these characteristic features recognized in the  $\tilde{E}-\tilde{A}$  excitation spectra, we can conclude that the energy region of IPS probed lies just below the photodissociation threshold correlating to NO( $E^2\Sigma^+$ ) + Ar.

The saturation experiments allowed us to search a much wider energy range of IPS of the NO( $E^2\Sigma^+$ )–Ar complex. Figures 3 (b) and (c) show the  $\tilde{E}-A$  (0, 0<sup>0</sup>, 0) excitation spectra of NO–Ar under unsaturated and saturated  $\nu_2$  laser power conditions, respectively. The saturated spectrum (Fig. 3 (c)) covers four times wider energy range of IPS as the unsaturated one (Fig. 3 (b)), while the highest energy limit of the saturated spectrum was almost the same as that of the unsaturated one. The saturation effect made the Franck-Condon region wider not only on the lower energy side, but also on the higher energy side of the unsaturated spectrum. Thus, the fact that the intensity of the peaks of the saturated spectrum suddenly falls off around 60950 cm<sup>-1</sup>, can be interpreted by that the dissociation threshold (NO( $E^2\Sigma^+$ ) + Ar) is 60950 cm<sup>-1</sup>. This value agrees with the dissociation threshold of 60951 cm<sup>-1</sup> estimated from the origin of uncomplexed NO (60863 cm<sup>-1</sup>) and the binding energy for the  $\tilde{X}$  state (88 cm<sup>-1</sup>). This evidence provides the reliability of the binding energy estimated previously [10].

The complexity of the vdW mode progression is astonishing. It seems that many bending structures are built on the stretching progression. The deep IPS of NO( $E^2\Sigma^+$ )–Ar would be more anisotropic, where the bending motion of the complex may behave like a normal mode bending vibration. If the complex in the  $\tilde{E}$  state is T-shaped, the accessible bending level may be restricted to one or two levels by the Franck-Condon principle, due to the T-shaped geometry of the complex in the ground state [9].

One plausible reason for this complexity is that the 4s $\sigma$  Rydberg orbital is not a pure s orbital. According to the quantum mechanical calculation [12], ns $\sigma$  and nd $\sigma$  Rydberg orbitals strongly mixed with each other except for 3s $\sigma$ . The 3s $\sigma$  Rydberg state has 94% pure s orbital character, although the 4s $\sigma$  state has 61% s, 1% p, and 39% d orbitals. Due to the d orbital character, we cannot treat the 4s $\sigma$  orbital as isotropic and the orientation of the 4s $\sigma$  orbital should be considered. The rotational structure becomes complex because the Hamiltonian includes the orientation effect with respect to the plane of three atoms [13]. For the same reason, the intermolecular vibrational structure also becomes complex [11]. To obtain detailed information on the intermolecular vibration, the rotationally resolved high-resolution spectrum is desired to be measured.



**Table 2** Molecular constants of NO-Ar complexes.

<i>state<sup>a</sup></i>	<i>T<sub>0</sub>(cm<sup>-1</sup>)</i>	<i>ω<sub>sr</sub>(cm<sup>-1</sup>)</i>	<i>D<sub>0</sub>(cm<sup>-1</sup>)</i>	<i>R<sub>vdW</sub>(Å)</i>
X <sup>2</sup> Π	0	–	88	3.7 <sup>b</sup>
A <sup>2</sup> Σ <sup>+</sup> (3sσ)	44242	~30	44	4.6
E <sup>2</sup> Σ <sup>+</sup> (4sσ)	60366	~80	585	–

<sup>a</sup> The electronic states are denoted by the NO molecular orbital character. The Ar atom is in the ground state (<sup>1</sup>S<sub>0</sub>).

<sup>b</sup> From Ref. 9

## References

1. M.-C. Duval, O. B. D'Azy, W. H. Breckenridge, C. Jouvét, and B. Soep, *J. Chem. Phys.*, **85**, 6324, 1986.
2. M. Okunishi, K. Yamanouchi, K. Onda, and S. Tsuchiya, *J. Chem. Phys.*, **98**, 2675, 1993.
3. J. M. Hutson, *Annu. Rev. Phys. Chem.*, **41**, 123, 1990; and references therein.
4. M. C. Heaven, *J. Phys. Chem.*, **97**, 8567, 1993; and references therein.
5. R. Engleman, Jr. and P. E. Rouse, *J. Mol. Spectrosc.*, **37**, 240, 1971.
6. R. Engleman, Jr., P. E. Rouse, H. M. Peek, and V. D. Baiamonte, Los Alamos Scientific Laboratory Report LA-4364.
7. C. Amiot and J. Verges, *Chem. Phys. Lett.*, **66**, 570, 1979.
8. P. R. R. Langridge-Smith, E. Carrasquillo M., and D. H. Levy, *J. Chem. Phys.*, **74**, 6513, 1981.
9. P. D. A. Mills, C. M. Western, and B. J. Howard, *J. Phys. Chem.*, **90**, 4961, 1986.
10. K. Tsuji, K. Shibuya, K. Obi, *J. Chem. Phys.*, **100**, 5441, 1994.
11. M.-L. Dubernet, D. Flower, and J. M. Hutson, *J. Chem. Phys.*, **94**, 7602, 1991.
12. K. Kaufmann, C. Nager, and M. Jungen, *Chem. Phys.*, **95**, 385, 1985.
13. W. M. Fawzy and J. T. Hougen, *J. Mol. Spectrosc.*, **137**, 154, 1989.